

THEORETICAL AND EXPERIMENTAL INVESTIGATIONS OF AERODYNAMICS AND FLIGHT DYNAMICS FOR MICRO-UAVS

Vladimir Brusov, Vladimir Petruchik, Yury Tiumentsev
Moscow Aviation Institute (MAI), Moscow, Russia

Keywords: *aerodynamics, flight dynamics, micro-UAV, hysteresis, simulation*

Abstract

Some special features are discussed for aerodynamics and flight dynamics of very small unmanned aerial vehicles (micro-UAV) as well as evaluation problems for aerodynamic and dynamic characteristics associated with these features. Some experimental results are presented for micro-UAV obtained by using wind tunnel experiments and flight tests as well as mathematical modeling results to estimate micro-UAV transient processes caused with some disturbances.

Nomenclature

- m – mass of UAV
- ρ – mass air density
- S – wing area of UAV
- c – mean aerodynamic chord
- U – flow velocity within a wind tunnel;
airspeed
- H – altitude
- q – dynamic head
- Re – Reynolds number
- α – angle of attack
- C_L – lift coefficient
- C_D – drag coefficient
- C_N – general force coefficient
- C_m – pitching moment coefficient
- μ – relative density
- $\bar{\tau}$ – time ratio
- p – angular velocity about X-axis
- q – angular velocity about Y-axis
- r – angular velocity about Z-axis
- I_Y – pitching-moment inertia
- σ_U – speed stability index

1 Introduction

A class of very-small unmanned aerial vehicles (micro-UAVs) including UAVs with a mass in the range from several dozen grams up to 1 kg (or up to 5 kg according to other appraisals) was emerged in the 90s due to formation of new technological possibilities to implement such kind of vehicles.

However micro-UAV design is a very difficult problem due to lack of appropriate theory of flight for such kind of objects. The point is that the micro-UAVs are much more similar to birds and insects than to conventional aircraft including larger UAVs (see Table 1) in terms of mass, dimensions, relative density, airspeed, Reynolds number values. We have no adequate analytical or numerical techniques to describe micro-UAV motion taking into account peculiarities mentioned above. This complicated problem remains still unsolved for modern aerodynamics and flight dynamics. On the other hand conventional theory of flight based mainly on empirical-type relationships reproducing long-term experience in design of ‘large’ aircraft does not specify flight of living beings as well as very small UAVs.

2 Some special features of micro-UAV motion

As can be seen from Table 1 mass m , relative density $\mu = 2m/\rho Sc$ and time ratio $\bar{\tau} = 2m/\rho SU$ for micro-UAV are much smaller than for manned aircraft and for larger UAVs. Here following designations are accepted: ρ is mass air density, S is wing area of UAV, c is mean aerodynamic chord, U is airspeed. On the

contrary, specific pitch moment values $M_{spec} = qSb / I_Y$ are dozens times more for micro-UAVs in comparison with larger aircraft. From this it

follows some specific features of motion nature for micro-UAVs:

Table 1
Some features for various kinds of flying objects

| Object kind | Mass m , kg | Re | Relative density, μ | Specific pitch moment, M_{spec} , 1/sec ² | Time ratio, sec |
|--------------------------------|---------------|-------------------------------|-------------------------|--|-----------------|
| Sporting airplanes and gliders | 500-1200 | $6 \cdot 10^5 - 10^7$ | 70-200 | 8-20 | 1.0-5.0 |
| Middle-sized UAV | 50-150 | $3 \cdot 10^5 - 10^6$ | 100-300 | 20-40 | 0.5-3.0 |
| Micro-UAV | 0.15 – 0.35 | $5 \cdot 10^4 - 2 \cdot 10^5$ | 20-40 | 200-1000 | 0.2-0.5 |
| Albatross | 8-12 | $2 \cdot 10^5 - 4 \cdot 10^5$ | 80-100 | 25-50 | 0.5-2.0 |
| Sea-gull | 0.8-2.0 | 10^5 | 60-80 | 60-120 | 0.5-2.0 |
| Butterfly | 0.0005-0.01 | $2 \cdot 10^3 - 8 \cdot 10^3$ | 2-6 | 2000-10000 | 0.01-0.06 |

1. Atmospheric disturbances are not only comparable with baseline in-flight forces influencing on the UAV but often exceed these forces.
2. Damping forces and moments are often similar in magnitude with baseline ones that provides rather fast attenuation of arising oscillations.
3. Angular velocities and angular accelerations of UAVs can reach very large values. This circumstance limits (though does not excludes completely) usage of stationary aerodynamic characteristics in flight dynamics problems for such vehicles.
4. Low-air-speed operating micro-UAVs are in the region of so-called critical Reynolds number values. Fast, practically stepwise variations of UAV aerodynamic characteristics are typical for this region. These variations influence immediately on the UAV motion, its stability and controllability.

All of these features dictate a need to improve baseline hypothesis, assumptions and models of motion as applies to micro-UAV. In turn, such improvements will be impossible without appropriate experiments basing on modern techniques and tools because of significance of the practice both as the basis for theoretical models and as validation criterion for used techniques. Certainly, this statement is fair for the UAV motion case as well.

Some results of experimental and theoretical research carried out by the authors in the recent

years are discussed in the subsequent sections of the paper.

3 Non-steady aerodynamic characteristics of micro-UAVs

Concerning unsteady aerodynamic characteristics some results are presented basing on wind tunnel tests to demonstrate Reynolds number influence on aerodynamic characteristics of a rectangular micro-UAV wing with the NACA-60 airfoil. Wing span was 500 mm and chord value was 80 mm in these experiments. A specific measurement technique (it was the Schmitz measurement technique [7]) has been used in the wind tunnel investigations. According to the technique wind tunnel flow velocity values (and Reynolds number values as a consequence) are changed at appropriate fixed values for angle of attack. The hysteresis phenomenon is revealed for micro-UAV aerodynamic characteristics depending on the Reynolds number while its values vary in ‘forward’ and ‘backward’ direction through the region of critical Reynolds number values.

Hysteresis appearance description in the form of ambiguous relationships for such static aerodynamic characteristics as experimentally defined general aerodynamic force and moment is presented in [4–7]. However these articles contain only qualitative discussion of rate of change for various kinematic parameters but they do not specify quantitatively the rates.

Therefore it is necessary to carry out specific research which allows us to make more exact physical understanding of aerodynamic phenomena caused with change of kinematic motion parameters such as velocity, angle of attack, angle of sideslip for a broad range of their values. Besides we need to study an influence of the phenomena on micro-UAVs aerodynamic characteristics as well as on their stability and control. Such extension of understanding is required to derive efficient supervision and control techniques for rapid and unstable processes relating to micro-UAV motion.

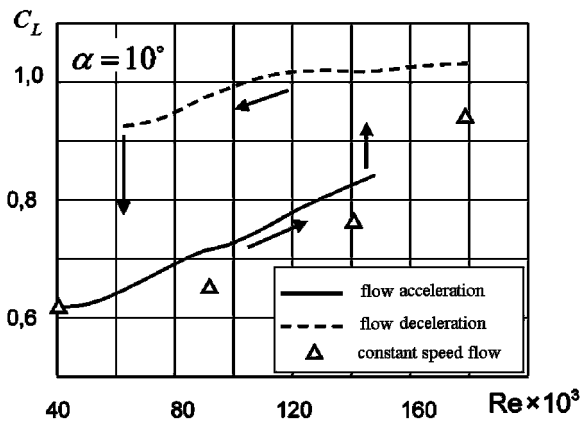


Fig. 1. Relationship $C_L(Re)$ for $\alpha = 10^0$

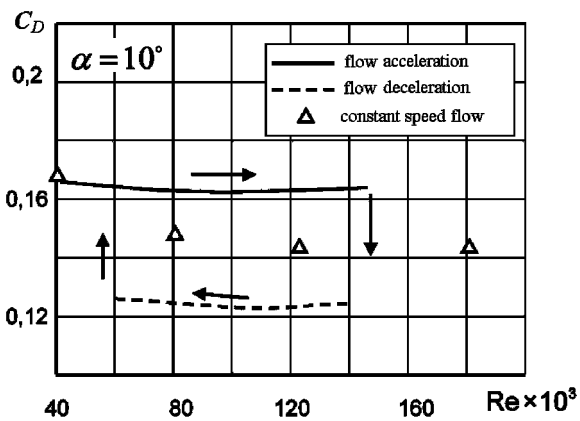


Fig. 2. Relationship $C_D(Re)$ for $\alpha = 10^0$

Relationships between C_L , C_D , C_m and Re obtained experimentally for angle of attack value $\alpha = 10^0$ are presented on Figs. 1–3. For all of these experiments carried out for angle of attack values from -10^0 to 20^0 flow velocity within wind tunnel increases initially with ac-

celeration $\dot{V} = 1,18 \text{ m/s}^2$ and then decreases with the same rate. Arrows on Figs. 1–3 indicate direction changes for Reynolds number values with respect to a specified rate of velocity change.

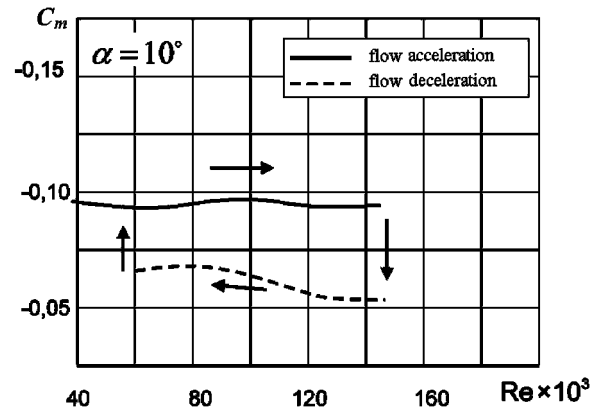


Fig. 3. Relationship $C_m(Re)$ for $\alpha = 10^0$

Aerodynamic wing polars and relationships $C_L(\alpha)$ are presented on Figs. 4 and 5 for three Reynolds number values $Re = 44000$, 62000 , 124000 , which were obtained by processing relationships $C_L(Re)$ и $C_D(Re)$ for angle of attack values from -10^0 to 20^0 . Behavior of polars and two hysteresis loops is demonstrated on Fig. 6 depending on values of Re , C_L and C_D parameters. The a,b,c,d loop arises here as velocity increases due to inertia of flow structure alteration within area of critical Reynolds number values.

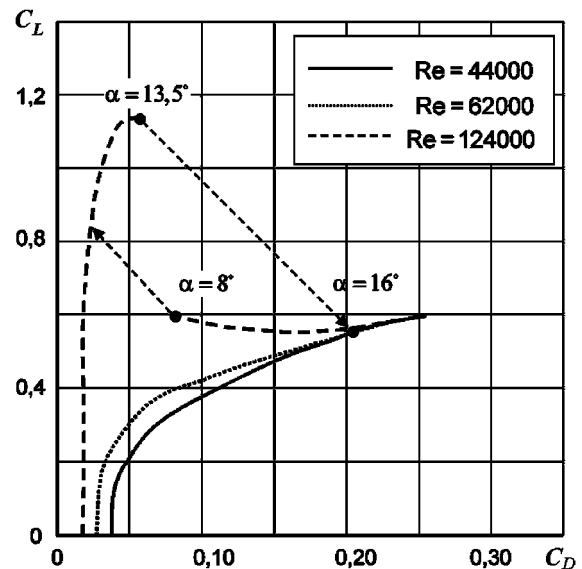


Fig. 4. Wing polars for $Re = 44000$, 62000 and 124000

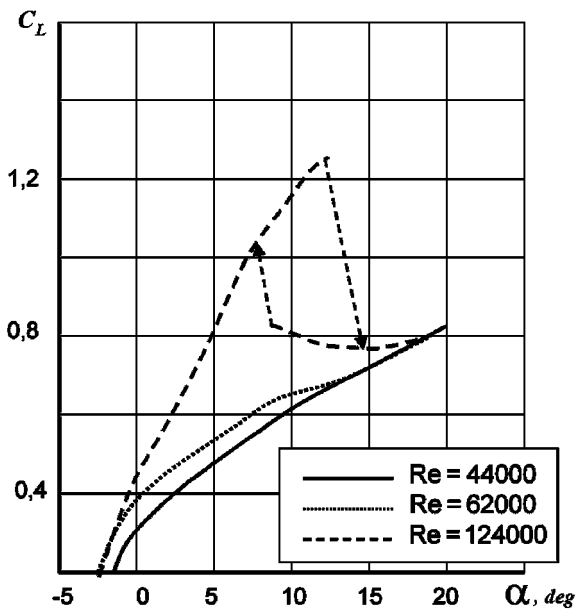


Fig. 5. Relationships $C_L(\alpha)$ for $Re = 44000$, 62000 and 124000

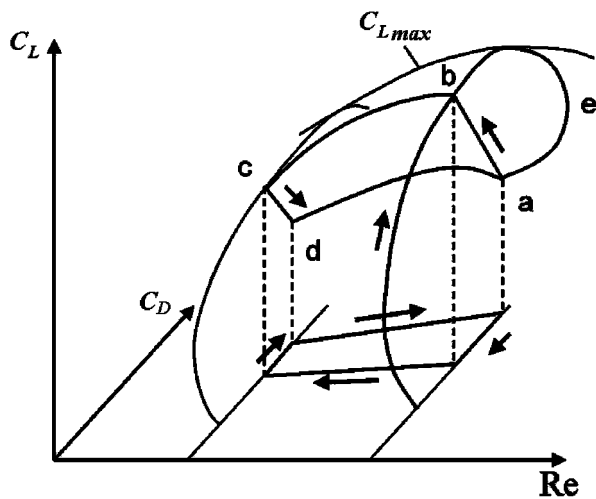


Fig. 6. Polars in space with Re , C_L , C_D coordinates and two hysteresis loops

4 Investigation of non-steady airflow around a micro-UAV wing

Wind tunnel investigations of non-steady wing aerodynamic characteristics with respect to angle of attack changing values were carried out using a special mounting (see Fig. 7). A distinctive feature of the mounting consists in modeling support for rotational wing movements with respect to various instantaneous centers of rotation. A six-component strain gage balance with

torque sensor was used to measure wing aerodynamic characteristics.

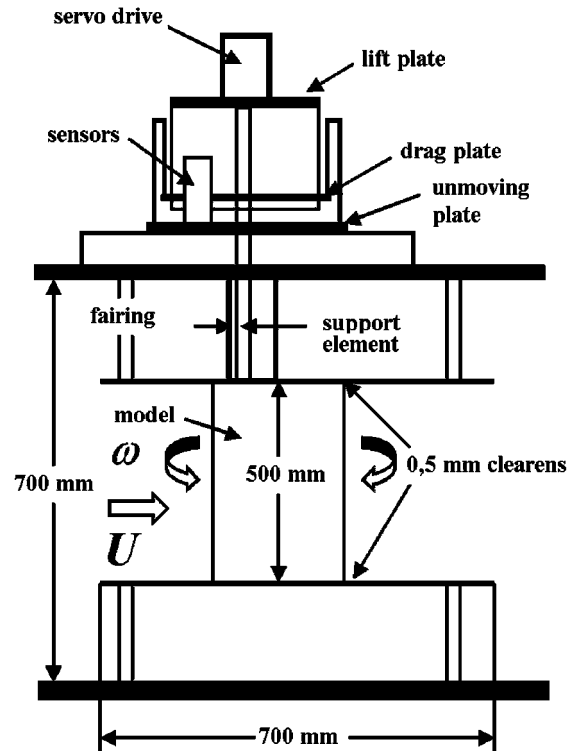


Fig. 7. Mounting scheme providing rotational freedom degrees for a wing model in wind tunnel

An essence of the experiment implemented using the test bench shown on Fig. 7 consists in measurement of general aerodynamic force represented with C_N coefficient values with respect to angle of attack changed continuously. The angle of attack values was varied in these experiments by means of constant-speed rotation for the wing model with respect to some instantaneous center of rotation.

Experimental results demonstrating influence of angular velocities and a location of instantaneous center of rotation on wing aerodynamic characteristics are presented on Figs. 8 – 12. Here $\bar{\omega} = \frac{\omega \cdot c}{2U}$ designates dimensionless an-

gular velocity with respect to some arbitrary center of rotation, ω is angular velocity with respect to some arbitrary center of rotation, c is wing chord and U is airflow velocity.

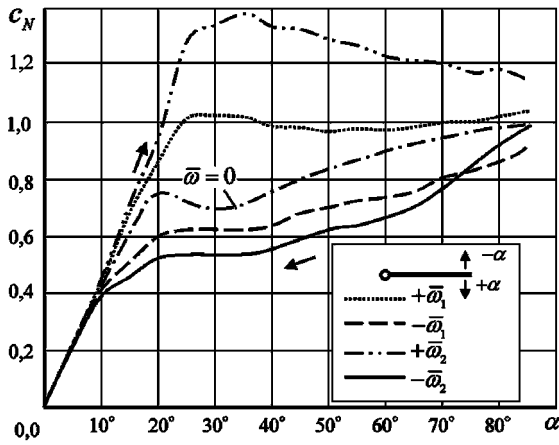


Fig. 8. Relationships $C_N(\alpha)$ for angular velocities $\bar{\omega}_1 = \pm 0.0131$ and $\bar{\omega}_2 = \pm 0.0393$ with respect to leading edge

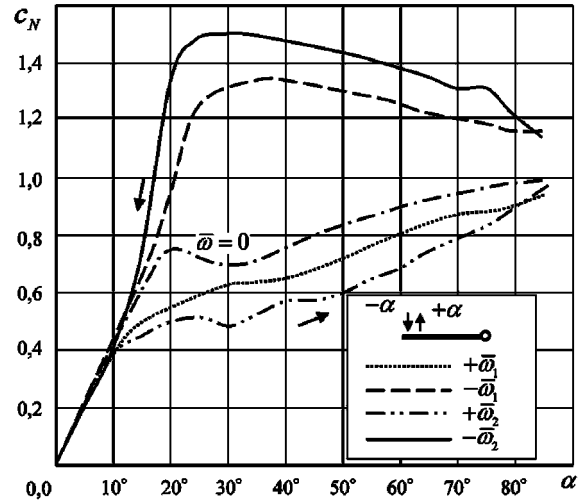


Fig. 11. Relationships $C_N(\alpha)$ for angular velocities $\bar{\omega}_1 = \pm 0.0131$ and $\bar{\omega}_2 = \pm 0.0393$ with respect to trailing edge

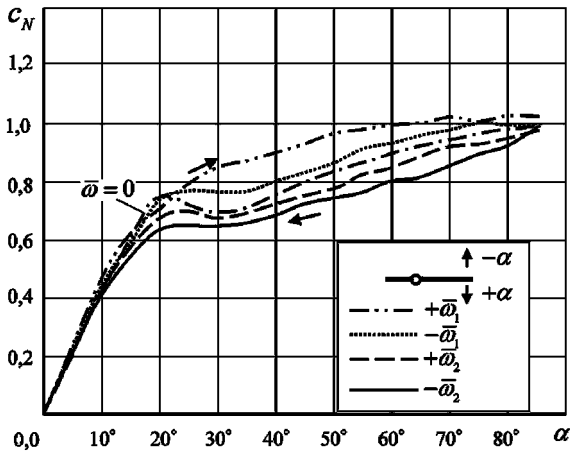


Fig. 9. Relationships $C_N(\alpha)$ for angular velocities $\bar{\omega}_1 = \pm 0.0131$ and $\bar{\omega}_2 = \pm 0.0393$ with respect to 0.25 of chord

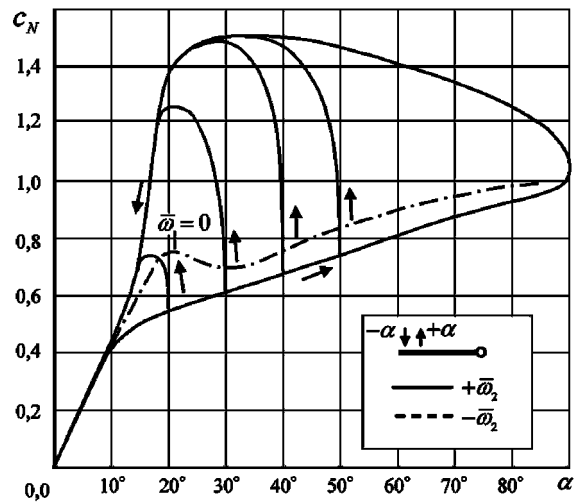


Fig. 12. Relationships $C_N(\alpha)$ for angular velocities $\bar{\omega}_1 = \pm 0.0131$ and $\bar{\omega}_2 = \pm 0.0393$ with respect to trailing edge depending on the switch point for direction of rotation

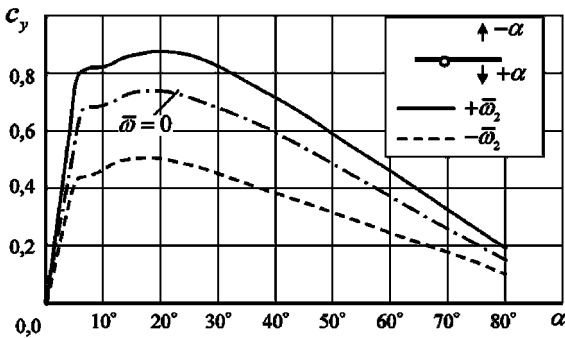


Fig. 10. Relationships $C_D(\alpha)$ for angular velocities $\bar{\omega}_1 = \pm 0.0131$ and $\bar{\omega}_2 = \pm 0.0393$ with respect to 0.25 of chord

These experimental results demonstrate significant influence of angular velocities and instantaneous center of rotation coordinates on aerodynamic characteristics for lifting surfaces. Such relationships need to be studied by means of elaborate investigation of theoretical and experimental aspects related to this research area.

5 Wind tunnel and flight investigation of aerodynamic characteristics for micro-UAVs

Experimental investigation results are presented in this section as applies to aerodynamic characteristics for some prototype micro-UAVs. These investigations were carried out by using the T-1 wind tunnel (see Fig. 13) installed in the Aerodynamic Laboratory at the Moscow Aviation Institute (MAI).

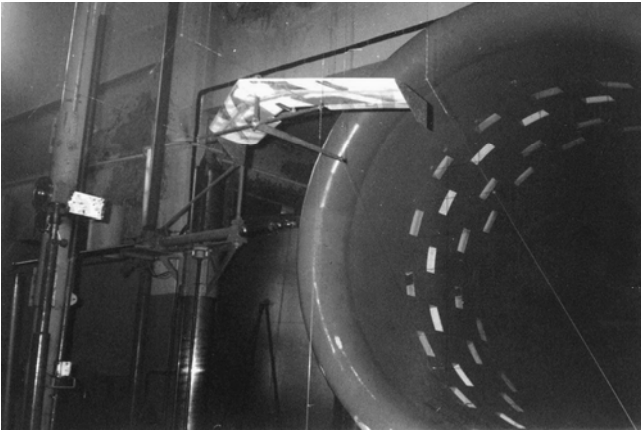


Fig. 13. Micro-UAV «002» within working section of the T-1 wind tunnel at the MAI

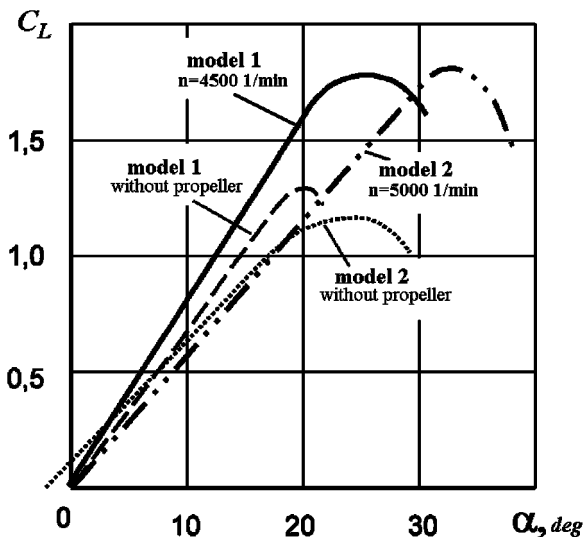


Fig. 14. Relationship $C_L(\alpha)$ for micro-UAV models No. 1 and 2

The subsonic T-1 closed-layout wind tunnel has an open working section with such main parameters as: output diameter of the contractor is 2.25 m, length of the working section is 3.4

m, range of operational flow velocities is from 5 m/sec to 50 m/sec, critical Reynolds number $Re = 3.5 \times 10^5$, initial turbulence degree is 0.35%.

Some results obtained in these experiments are presented on Figs. 14 through 17.

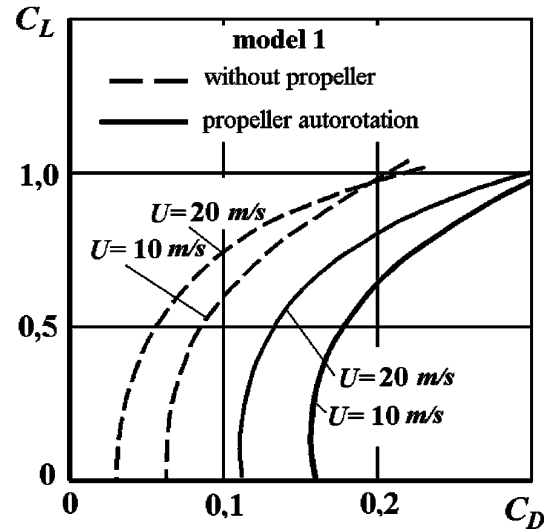


Fig. 15. Aerodynamic polars $C_L(C_D)$ for micro-UAV model No. 1

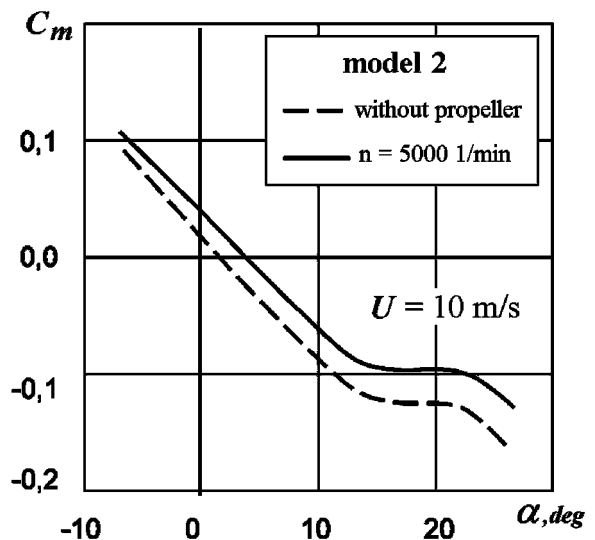


Fig. 16. Pitching moment coefficient $C_m(\alpha)$ for micro-UAV with and without operating propeller

Experiments were performed at values of Reynolds number which are typical for micro-UAVs including study with operating engines and propellers as well as with autorotating propeller and without propellers.

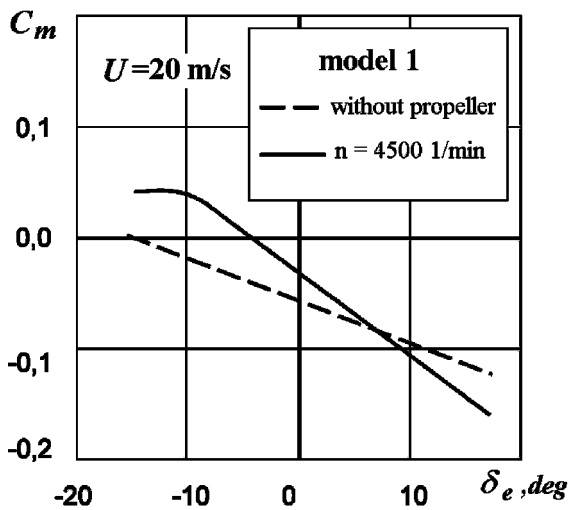


Fig. 17. Propeller blowing influence on longitudinal control efficiency for micro-UAV model No. 1

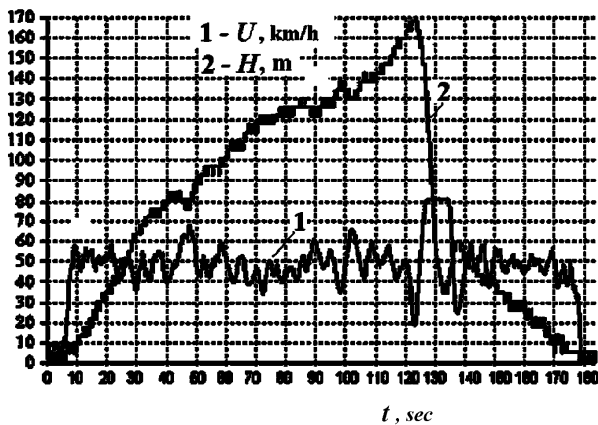


Fig. 18. Micro-UAV altitude and airspeed registered in flight tests

Flight test results are presented also in the article (see Figs. 18 and 19) for an experimental micro-UAV equipped with microprocessor-based registration system to record values of UAV flight parameters including airspeed U , barometric altitude H , deflections of control surfaces (angles of aileron ξ , rudder ζ and elevator η deflections), linear acceleration components a_x , a_y , a_z and angular velocity components p , q , r along X, Y, Z coordinate axes. These flight investigation results demonstrate in very convincing manner how fast micro-UAV flight parameters can be changed under atmospheric disturbances or under the action of deflected control surfaces. Especially angular velocities p , q , r vary their values considerably.

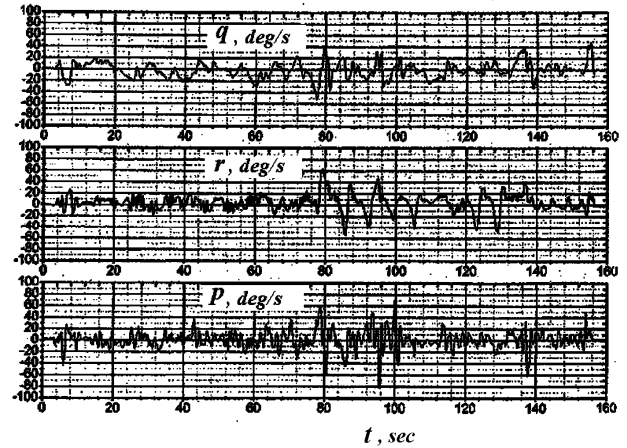


Fig. 19. Micro-UAV angular velocities registered in flight tests

6 Simulation of transient processes for micro-UAVs

Mathematical modeling and computer simulation were performed basing on experimental results to analyze the micro-UAV transition processes. The analysis was accomplished using linear and nonlinear models of disturbed motion [8]. Obtained numerical results show us that there are some peculiarities in longitudinal stability characteristics of micro-UAVs within region of critical Reynolds number values. It is possible particularly to loose the speed stability ($\sigma_U > 0$) for some value combinations of longitudinal trim parameters, aerodynamic center location and damping coefficient value.

A detailed analysis has been carried out within the framework of the linear model to obtain roots of characteristic equation for some micro-UAVs as well as comparison were made with roots for the Yak-18T light piloted aircraft equipped with a piston engine. The comparison demonstrates that micro-UAVs have several times larger natural oscillation frequencies than larger aircraft due to very small values of inertia moments and large values of specific pitch moment. In addition micro-UAVs have several times larger damping values caused with their small relative density values in longitudinal motion. For the rest, relationships describing changes of the root values remain very similar for micro-UAVs and piloted airplane within their operating ranges of airspeeds, which are certainly different for these classes of vehicles.

Simulation results are presented in the article concerning to transient processes in longitudinal micro-UAV motion. The results indicate that transitions for such angular motion variables as angle of attack α and pitch angular velocity q include some high-frequency and rapidly damped motion mode as well as a low frequency and relatively slow damped one.

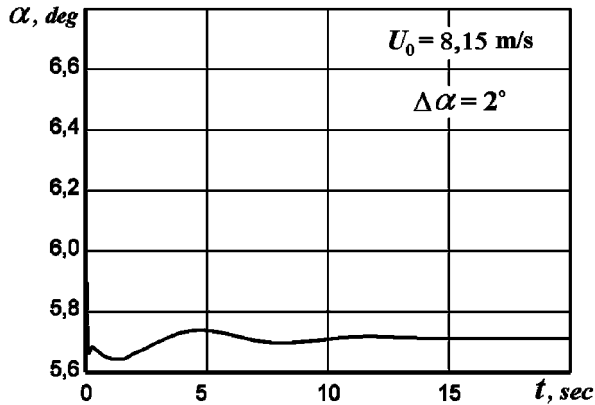


Fig. 20. Transient process for angle of attack $\alpha(t)$ caused with $\Delta\alpha = 2^\circ$ initial disturbance

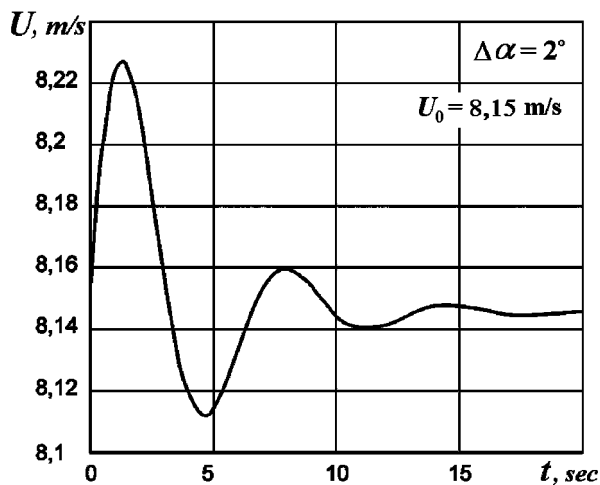


Fig. 21. Transient process for airspeed $U(t)$ caused with $\Delta\alpha = 2^\circ$ initial disturbance for the angle of attack value

There are also transient processes related to changing flight path variables such as airspeed U and flight path angle γ , which have no high-frequency mode (Figs. 20 and 21).

Simulation results are presented on Figs. 20 and 23 to demonstrate transient processes for the X-04 micro-UAV in regard to their angular and flight path movements. These results have been obtained using nonlinear model of aircraft spatial motion.

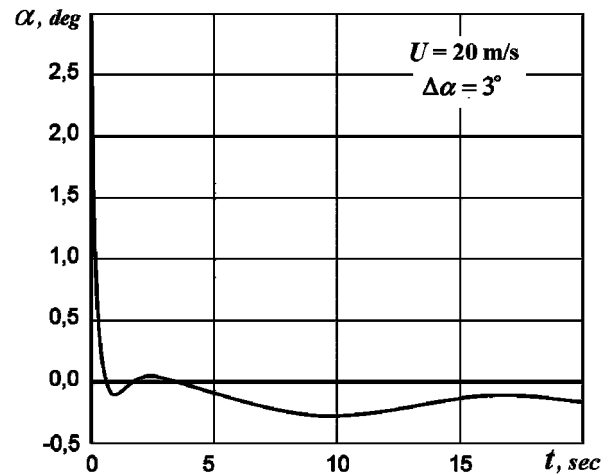


Fig. 22. Transient process for angle of attack $\alpha(t)$ caused with $\Delta\alpha = 3^\circ$ initial disturbance

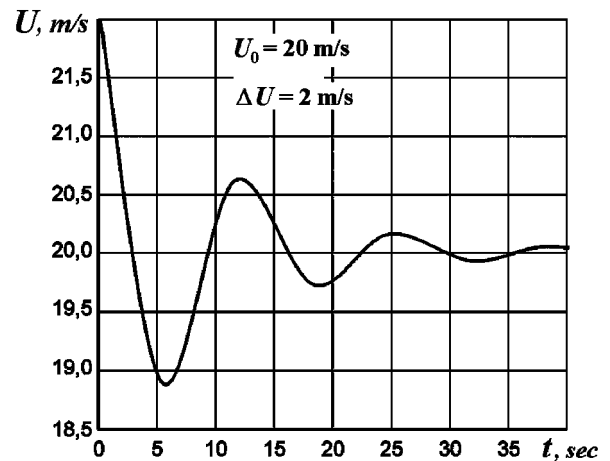


Fig. 23. Transient process for airspeed $U(t)$ caused with $\Delta V = 2$ m/s initial disturbance

Comparison of simulation results basing on linear and nonlinear models demonstrates that these models lead to a close agreement in their results if initial disturbances are small. However the linear model (it is inherently analytical) has an important benefit because it allows us to analyze roots of characteristic equation for the investigated system. It is possible using the analysis results to make conclusions about an influence degree of micro-UAV parameters on a kind of transition processes. On the other hand nonlinear model (it is inherently numerical and simulation-based) of the disturbed motion produces more accurate results and can operate not only for small disturbances but for large ones. It is profitable for practical applications to use these two kinds of models in some joint mutually complementary manner.

7 Conclusions

The results of theoretical and experimental investigations described in previous sections indicate clearly that micro-UAVs have some important features which are absent for bigger and faster aircraft. One of these features is presence of hysteresis loop in many aerodynamic characteristics such as lift, drag and pitching moment coefficients for longitudinal motion of micro-UAV. Other special micro-UAV features discussed above relate to non-steady and nonlinear motion nature of these vehicles. Such features impact significantly on micro-UAVs stability and control characteristics and therefore they are needed to take into account while designing micro-UAVs and their control systems.

References

- [1] Brusov V.S. and Petruchik V.P. Theoretical and experimental investigations of aerodynamic characteristics for micro-UAV. *Proc. 3rd US-European Competition and Workshop on Micro Air Vehicle Systems (MAV07) & European Micro Air Vehicle Conference and Competition (EMAV2007)*, 17-21 September 2007, Toulouse, France.
- [2] Brusov V.S. and Petruchik V.P. Aerodynamics and flight dynamics for small unmanned aerial vehicles. *Proc. XXI Scientific Conference on Aerodynamics*, TsAGI Publishing Department, 2010 (In Russian).
- [3] *Aerodynamics stability and handling qualities for supersonic airplanes* / Ed. by Biushgens, Moscow, Fizmatlit, 1998 (In Russian).
- [4] Kurianov A.I., Stoliarov G.I., Steinberg R.I. About hysteresis of aerodynamic characteristics. *TsAGI Academic Transactions*, vol.10, No. 3, 1979 (In Russian).
- [5] Begovshits V.N., Kabin V.N., Kolinko K.A. a.o. Free oscillation on elastic joint technique to study non-stationary transonic aerodynamic derivatives. *TsAGI Academic Transactions*, vol.27, No. 3-4, 1996 (In Russian).
- [6] Kolin I.V., Mamrov V.P., Sviatodukh V.K. a.o. Multiple hysteresis of steady aerodynamic characteristics for aeroplane with a high-aspect-ratio straight wing on low Reynolds number values. *TsAGI Preprint*, No. 87, 1996 (In Russian).
- [7] Schmitz F.W. *Aerodynamik des Flugmodells*. 2. Aufl., Carl Lange Verlag, Duisburg, 1952.
- [8] *Aeromechanics of airplane: Flight dynamics* / Ed. by A.F. Bochkariov and V.V. Andreyevsky, 2nd Ed., Moscow, Mashinostroyeniye, 1985 (In Russian).

Contact Author Email Address

tium@mai.ru

Yury Tiumentsev, Ph.D., Principal Research Associate and Associate Professor at the MAI

Copyright Statement

The authors confirm that they, and/or their company or organization, hold copyright on all of the original material included in this paper. The authors also confirm that they have obtained permission, from the copyright holder of any third party material included in this paper, to publish it as part of their paper. The authors confirm that they give permission, or have obtained permission from the copyright holder of this paper, for the publication and distribution of this paper as part of the ICAS2010 proceedings or as individual off-prints from the proceedings.